Journal of Applied Mechanics and Technical Physics, Vol. 42, No. 6, pp. 1078–1082, 2001

STATIC CRACK RESISTANCE OF IRON-BASED SINTERED POWDER MATERIALS

A. V. Fedotov

UDC 539.55:620.1

A boundary-value problem of static crack resistance of structurally heterogeneous sintered materials is formulated within the framework of the structurally phenomenological approach. A numerical algorithm for modeling the mechanical behavior of structurally heterogeneous cracked powder materials is proposed. Crack resistance of some structurally heterogeneous powder materials is estimated. The anomalous character of the crack resistance revealed is studied with the use of fractography. Theoretical findings are supported by results of mechanical cracking tests.

Introduction. Progress in science and engineering is closely related to the wide use of materials produced in powder metallurgy [1–4]. Powder materials are used in structures operating under extreme loading conditions. In some cases, a structure fails because of the presence and growth of cracks [5–6]. To ensure safety and operating capacity of a cracked structure, it is necessary to know characteristics of fracture toughness of the material used [7].

In some cases, it is impossible to estimate the operating capacity of a structure; therefore, laboratory tests of specimens made of the same material as the structure are performed. In view of limited potentialities of experimental methods of investigating the crack resistance of structurally heterogeneous powder materials, the present work is urgent.

1. Experimental Study. As a subject of investigation, we considered iron-based sintered powder materials. An iron powder (OS.Ch.6-2) or a multicomponent mixture (based on iron, carbon, chromium, nickel, and molybdenum powders) was compacted in a closed mould at room temperature; the blanks were $90 \times 16 \times 16$ mm parallelepipeds. The powder was sintered at 1200°C in protective atmosphere (hydrogen) within 2 h for iron and 4 h for PK100N4M and ZhGr1.5Kh2N materials. Depending on compaction pressure, the residual porosity of the materials was 0.4–26.5% [8].

The specimens were produced from blanks shaped like parallelepipeds by mechanical treatment. Before testing, the specimens were loaded as cantilevered beams to obtain a fatigue crack at the tip of a V-shaped notch. Depending on the force applied to the specimens, the tests were performed on a 2055R-0.5 test machine with a maximum load of 500 kg or an R-10 machine for static tests with a maximum load of 10,000 kg. The deformation curves obtained were used to calculate the static crack resistance of functional powder materials.

To process experimental results, we use models of deformation and fracture mechanics of structurally heterogeneous macroisotropic materials and analyze the stress–strain state of a powder composite at the macroscopic level. We formulate the linear boundary-value problem of deformation and fracture of a specimen with a concentrator. The specimen occupies a two-dimensional domain D (Fig. 1) bounded by a closed contour whose configuration changes as the crack grows under loading. The following equations are valid in the domain D:

$$\sigma_{ij,j} = 0, \qquad \varepsilon_{ij} = (u_{i,j} + u_{j,i})/2, \qquad \sigma_{ij} = C_{ijkl}\varepsilon_{kl}.$$

Here σ_{ij} are the stress-tensor components, ε_{ij} are the strain-tensor components, u_i are the displacement-vector components, and C_{ijkl} is the elastic constant tensor. The boundary conditions have the form

$$\sigma_{ij}n_j = 0, \qquad u_i\Big|_{\mathrm{A,B}} = 0, \qquad u_1\Big|_{\mathrm{C}} = 0, \qquad u_2\Big|_{\mathrm{C}} = v. \tag{1.1}$$

Perm' State Technical University, Perm' 614600. Translated from Prikladnaya Mekhanika i Tekhnicheskaya Fizika, Vol. 42, No. 6, pp. 183–189, November–December, 2001. Original article submitted March 30, 2001; revision submitted July 9, 2001.

 0021-8944/01/4206-1078 $25.00

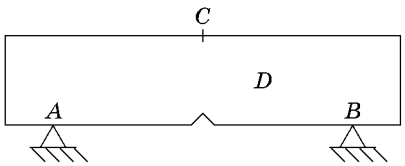

Fig. 1. Notched specimen.

Here v is the displacement (deflection) at the point C where the load is applied and n_j are the components of the outward normal to the surface. The first condition in (1.1) is satisfied everywhere on the boundary of the domain D except for points A, B, and C.

The problem of an equilibrium crack is solved by the boundary-element method, which leads to the system of governing equations

$$A\boldsymbol{g} = B\boldsymbol{G}, \tag{1.2}$$

where A and B are the matrices of the boundary-influence coefficients and $\boldsymbol{g}$ and $\boldsymbol{G}$ are the global vectors of boundary displacements and forces with some components known. Once system (1.2) is solved, one can determine stresses and displacements at the surface of the body and, hence, calculate the force vector at an arbitrary point of the surface:

$$\boldsymbol{F}\boldsymbol{r}_i = \sigma_n S.$$

Here σ_n is the normal stress on the body surface and S is the area of the site where the stress σ_n acts.

Initially, failure does not occur in the body and the length of the crack is equal to zero. Using the Clapeyron theorem, we express the elastic energy of the body in terms of the boundary stresses and displacements, some components of which are determined from the boundary conditions (1.1) and the remaining components are dependent quantities determined from system (1.2):

$$W_0 = 0.5 \int (u_s\sigma_s + u_n\sigma_n)\, dS. \tag{1.3}$$

Here u_s and u_n are the tangential and normal boundary displacements, respectively, and σ_s and σ_n are the shear and normal boundary stresses, respectively.

In experiments, the elastic energy was determined by the formula

$$W_i = 0.5 \int (u'_s\sigma'_s + u'_n\sigma'_n)\, dS, \tag{1.4}$$

where u'_s and u'_n are the tangential and normal boundary displacements, respectively, and σ'_s and σ'_n are the shear and normal boundary stresses, respectively.

Using the well-known relations of fracture mechanics, we express the crack resistance in terms of the intensity of released energy as

$$G = -dW/dl \approx \Delta W/\Delta l, \tag{1.5}$$

where $\Delta W = W_i - W_0$ and $\Delta l = l_i - l_0$, and calculate the stress intensity factor

$$K_{\mathrm{I}} = \sqrt{GE/(1-\mu^2)}, \tag{1.6}$$

where E and μ are the effective elastic constants of the powder material.

The experimental data were processed by the numerical algorithm proposed by Sokolkin et al. [9]. The experimental values of the fracture toughness of sintered materials are listed in Table 1.

2. Fractography Analysis. Figure 2 shows the crack resistance versus the porosity of specimens from a structurally heterogeneous powder material PK100N4M prepared by the method outlined in Sec. 1. The curve is not monotonic in contrast to the monotonic dependences of strength and elasticity on porosity. The minimum crack resistance of the PK100N4M, ZhGr1.5Kh2N, and OS.Ch.6-2 materials is obtained for porosity within 5–9%. The dependences obtained by processing experimental data can be written in the general form $\chi = \chi_0(1-\Theta)^m$, where χ is a certain characteristic of the porous material, χ_0 is the same characteristic of the pore-free material, Θ is the volume fraction of pores, and m is a coefficient which takes different values for different characteristics

TABLE 1

Material	$K_{\mathrm{I,cr}}$, MPa · m$^{1/2}$		
	Experiment	Calculation under the assumption of macrohomogeneity	Calculation under the assumption of heterogeneity
PK100N4M	73.9–100.5	81.6–108.8	—
ZhGr1.5Kh2N	68.5–85.2	74.9–92.8	—
OS.Ch.6-2	25.2–38.9	27.1–43.1	28.0–44.4

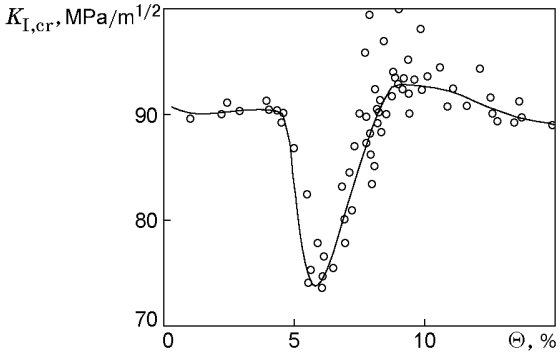

Fig. 2. Effect of porosity on the crack resistance of the PK100N4M powder material.

(for example, $m = 3$–6 for strength). The dependence of the crack resistance of structurally heterogeneous porous materials on the volume fraction of pores has the form

$$K_{\mathrm{I,cr}} = a(1 - \Theta)K^0_{\mathrm{I,cr}} + b\Theta\sigma\sqrt{\xi},$$

where a and b are constants, $K^0_{\mathrm{I,cr}}$ is the critical stress-intensity factor, σ is the strength of the pore-free material, and ξ is the average diameter of the pores.

To study the microstructure of a fracture surface, we performed a fractography analysis using an SCANNEX IIc scanner and a computer for automatic digitization and recording of results. In fractography, it is important to preserve the fracture surface. If the fracture surfaces are subjected to a mechanical or chemical action, the fractography analysis gives unreliable results. Therefore, we examined the fracture surfaces of specimens immediately after experiment. A careful fractography analysis was performed for the fracture surfaces of all specimens tested for crack resistance, including those made of the ZhGr1.5Kh2N powder steel with a porosity of 1.6–15.1%, PK100N4M powder steel with a porosity of 1.1–14.9%, and OS.Ch.6-2 powder material with a porosity of 0.4–26.5%.

Figure 3 shows the microstructure of the fracture surface of a specimen from the OS.Ch.6-2 powder material with a porosity $\Theta \approx 2\%$. Several zones can be distinguished in the structure of all the powder materials tested. Fracture begins from the notch and propagates at an angle to the specimen axis (zone 1). It should be noted that the size of this zone depends on the plastic properties of the material. The maximum size is observed for the OS.Ch.6-2 material. Zone 2 lies in the plane normal to the specimen axis; it is a part of the detachment surface. The lateral slopes (zone 3) and final-fracture region (zone 4) located at an angle of 45° to the specimen axis are formed under the action of shear stresses.

The common feature of the microstructures of the tested specimens from the PK100N4M, ZhGr1.5Kh2N, and OS.Ch.6-2 materials is that the fracture occurs by spalling regardless of their porosity. It is noteworthy that the fracture surface of the specimens has a pit structure. The fraction of the fracture surface with a pit relief increases in proportion to the porosity of the material.

A certain difference in the structure of zones shown in Fig. 3 is observed. In zones 1, 3, and 4, there are parabolic pits typical of shear fracture, and there are strongly elongated pits on the surface of the lateral slopes (zone 3). There are regions of smooth delamination, which are also typical features of the microrelief under shear fracture. Zone 2 is characterized by parabolic pits of eccentric detachment and equiaxial pits of normal detachment. It should be noted that, as the carbon content in specimens increases, the number of quasi-spalling regions increases and their energy content decreases, which is pronounced for some tested specimens from the PK100N4M and

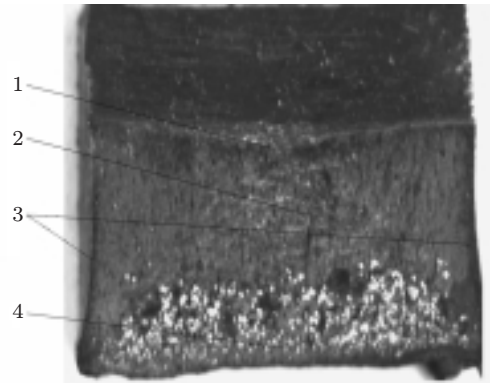

Fig. 3. Microstructure of the fracture surface of a specimen from the OS.Ch.6-2 powder material ($\Theta \approx 2\%$).

ZhGr1.5Kh2N powder materials. In these specimens, elements of intergranular fracture are clearly seen. The regions of brittle intergranular fracture observed are characteristic of specimens with $\Theta = 5$–9%. Brittle fracture of specimens with $\Theta < 5\%$ occurs over the grains (Fig. 3), which is caused by redistribution of impurities in powder materials with different porosities. For energy reasons, the impurity atoms tend to occupy the free surface of pores. Upon compaction of the material sintered and collapse of the pores, they enter the metal matrix. Initially, the impurity atoms are concentrated on intergrain boundaries. This increases the probability of brittle fracture over the grain boundaries. Therefore, regions of brittle intergranular fracture are expected to appear on the fracture surface. Further compaction of the material leads to a more uniform distribution of impurity atoms in the bulk of grains. In this case, the grains themselves become brittle, and fracture of the material has a transcrystallite character, which is supported by the results of fractography analysis (Fig. 3).

Fractography of the fracture surfaces of sintered powder specimens shows that the presence of flat pores decreases the crack resistance. However, this effect is small, since flat pores are not always formed, depending on the production technology of a material.

3. Numerical Modeling. To solve the problem of a crack propagating through a deformable body, one has to determine the stress–strain state of the latter. To this end, we used the ANSYS software package. The problem was solved by the finite-element method (the finite-element model included 6228 rectangular elements and 7749 nodes). The crack front was modeled by singular elements. The stress–strain state at the moment of fracture of a specimen from the PK100N4M material with the modulus of elasticity $E = 200$ GPa, Poisson's ratio $\mu = 0.27$, and porosity $\Theta = 9.4\%$ was calculated. The specimen was 90 mm long, 16 mm high, and 16 mm thick; the distance between the supports was 75 mm; the V-shaped notch was 4 mm deep. Using the calculation results, we determined the crack resistance of the powder material by formulas (1.5)–(1.8). The values of $K_{\mathrm{I,cr}}$ for the OS.Ch.6-2, ZhGr1.5Kh2N, and PK100N4M powder materials, obtained under the assumption of macroscopic homogeneity, are listed in Table 1.

In the neighborhood of cracks, the medium was assumed to be homogeneous. To refine and develop the theory of fracture, it is necessary to take into account the structure of the medium. As an example, we consider the OS.Ch.6-2 material. The mathematical formulation of the problem comprises the closed system of equations

$$\sigma_{ij,j}(\boldsymbol{r}) = 0, \qquad \sigma_{ij}(\boldsymbol{r}) = f_{ij}(a_{kl}(\boldsymbol{r}), \varepsilon_{kl}(\boldsymbol{r})), \qquad \varepsilon_{ij}(\boldsymbol{r}) = [u_{i,j}(\boldsymbol{r}) + u_{j,i}(\boldsymbol{r})]/2 \tag{3.1}$$

and the boundary conditions

$$u_i(\boldsymbol{r})\Big|_{\Gamma} = u_i^{(0)}(\boldsymbol{r}), \tag{3.2}$$

where $u_i^{(0)}(\boldsymbol{r})$ is the displacement vector specified at the surface Γ.

It is required to find the stress field $\sigma(\boldsymbol{r})$ satisfying the boundary-value problem (3.1) and the boundary conditions of the first kind (3.2). The boundary conditions are specific for each specimen; they are calculated under the assumption of macroscopic homogeneity of the material. The problem was solved by the finite-element method using the ANSYS software package (16,000 finite elements and 18,491 nodes were used). The crack front was modeled by singular elements. The normal and shear stresses were determined for a specimen with $E = 160$ GPa and $\mu = 0.26$.

We now study the relation between microscopic and macroscopic stress fields for structurally heterogeneous powder materials, using a widely accepted method based on averaging the smooth components of structural deformation fields [10]. In accordance with this method, the equations of the structurally phenomenological model are reduced to a system for averaged stresses, strains, and displacements, which are called macroscopic. Physically, one can relate the structural deformation variables to the macroscopic variables by using the concept of an elementary macrovolume [11, 12].

Using the algorithm proposed above, we calculated the macrocharacteristics of the material, in particular, the macrostress fields, and determined the coefficient $K_{\mathrm{I,cr}}$ of the OS.Ch.6-2 powder material by formulas (1.5)–(1.8). The critical stress-intensity factors $K_{\mathrm{I,cr}}$ listed in Table 1 were calculated with allowance for the inhomogeneous structure of the material and, therefore, are rather accurate.

4. Discussion of Results. Table 1 summarizes experimental and theoretical values of $K_{\mathrm{I,cr}}$ for the OS.Ch.6-2, ZhGr1.5Kh2N, and PK100N4M powder materials. The calculation results agree well with experimental data obtained by the method proposed above. The values of $K_{\mathrm{I,cr}}$ calculated in the two- and three-dimensional formulations for a homogeneous body differ by no more than 11.2%. A comparative analysis shows that the solution of the two-dimensional problem agrees satisfactorily with the solution of the three-dimensional problem with allowance for heterogeneity of the OS.Ch.6-2 material. The discrepancy in numerical results does not exceed 15.8%. It is obvious that the scatter in the results depends on structural heterogeneity of the material. For some specimens, however, the discrepancy was smaller than 2.6%. This can be explained by the low porosity of these specimens (0.4–2.8%). The solution of the three-dimensional problem shows that the maximum error in determining the stress-intensity factor of the material is 4.6% for specimens with high porosity. Thus, the discrepancy between the two- and three-dimensional solutions increases with the porosity of the material.

Conclusions. The method proposed allows determination of the static crack resistance of structurally heterogeneous powder materials. Using this method, one can readily estimate $K_{\mathrm{I,cr}}$ with a satisfactory accuracy in simple and rapid tests.

This work was supported by the Russian Foundation for Fundamental Research (Grant No. 99-01-00910).

REFERENCES

1. R. A. Andrievskii, *Powder Material Science* [in Russian], Metallurgiya, Moscow (1991).
2. V. B. Akimenko, V. Ya. Bulanov, V. V. Rukin, et al., *Iron Powders* [in Russian], Nauka, Moscow (1982).
3. A. N. Stepanchuk, I. I. Bilin, and P. A. Boiko, *Technology of Powder Metallurgy* [in Russian], Vishcha Shkola, Kiev (1989).
4. G. A. Libenson, *Fundamentals of Powder Metallurgy* [in Russian], Metallurgiya, Moscow (1987).
5. J. A. Collins, *Failure of Materials in Mechanical Design*, John Wiley and Sons, New York (1981).
6. V. Z. Parton, *Fracture Mechanics: From Theory to Practice* [in Russian], Nauka, Moscow (1990).
7. V. V. Bolotin, *Service Life of Machines and Structures* [in Russian], Mashinostroenie, Moscow (1990).
8. Yu. V. Sokolkin, A. V. Fedotov, and A. A. Chekalkin, "Experimental determination of the critical stress-intensity factor of the PK100N4M powder material," in: *Mathematical Modeling and Boundary-Value Problems*, Proc. IX Conf. (Samara, Russia, May 25–27, 1999), Samara (1999), pp. 178–182.
9. Yu. V. Sokolkin, A. V. Fedotov, and A. A. Chekalkin, "Experimental-calculation method for analysis of cracks propagating in structurally heterogeneous powder materials," *Vestn. Perm. Gos. Tekh. Univ., Mekh. Kompozit.*, No. 1, 100–105 (1999).
10. R. I. Nigmatulin, *Fundamentals of Mechanics of Heterogeneous Continua* [in Russian], Nauka, Moscow (1978).
11. L. Broutman and R. Crock (eds.), *Composite Materials*, Vol. 2: G. Sendeckyj, *Mechanics of Composite Materials*, Academic Press, New York (1974).
12. I. N. Bogachev, A. A. Vainshtein, and S. D. Volkov, *Introduction to Statistic Metal Science* [in Russian], Metallurgiya, Moscow (1972).